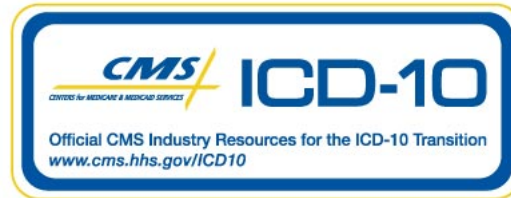


**GET HELP FROM
CMS HERE**



**Vascular morphometric changes after radioactivestent implantation: a
dose-response analysis**

Paul Wexberg, Christian Kirisits, Mariann Gyöngyösi, Michael Gottsauner-Wolf,
Meinhard Ploner, Boris Pokrajac, Richard Pötter, and Dietmar Glogar
J. Am. Coll. Cardiol. 2002;39;400-407

This information is current as of February 10, 2012

The online version of this article, along with updated information and services, is
located on the World Wide Web at:

<http://content.onlinejacc.org/cgi/content/full/39/3/400>

JACC

JOURNAL of the AMERICAN COLLEGE of CARDIOLOGY



Vascular Morphometric Changes After Radioactive Stent Implantation: A Dose-Response Analysis

Paul Wexberg, MD, BM,* Christian Kirisits, MSc, DSc,† Mariann Gyöngyösi, MD, PhD,*
Michael Gottsauner-Wolf, MD,* Meinhard Ploner, MSc,‡ Boris Pokrajac, MD,† Richard Pötter, MD,†
Dietmar Glogar, MD*

Vienna, Austria

OBJECTIVES	The goal of this study was to evaluate the dose-dependency of morphometric changes in the coronary arterial wall after radioactive stenting.
BACKGROUND	Radioactive stents have been found to reduce intrastent intimal hyperplasia (IIH) but lead to a characteristic type of restenosis occurring predominantly at the stent edges.
METHODS	Fifteen patients underwent intravascular ultrasound (IVUS) examination after implantation of a P-32 radioactive stent and at the six-month follow-up. The post-stent IVUS measurements on seven predefined locations of each lesion were subjected to a computer algorithm for the development of dose-volume histograms (DVH). Thus, we derived the radiation doses delivered to at least 10% and 90% of the adventitia (DV10, DV90). The IIH and vascular remodeling at follow-up were correlated with the doses in each segment.
RESULTS	The IIH was most pronounced at the stent edges and lowest in the stent-body, whereas we detected a significant expansive remodeling within the stent body. The delivered doses correlated with a decreased IIH ($r = 0.52$, $p < 0.001$ for DV10 and $r = 0.62$, $p < 0.001$ for DV90) and with expansive remodeling ($r = 0.48$, $p = 0.009$ for DV10 and $r = 0.50$, $p = 0.006$ for DV90). A DV10 >90 Gy or a DV90 >15 Gy reduced IIH and induced expansive remodeling. Plaque growth was not reduced by radioactive stents.
CONCLUSIONS	The DVH analysis reveals a dose-dependent increase of external elastic lamina area behind radioactive stents, whereas plaque growth is not reduced but inverted into an outward direction from the stent. A DV10 >90 Gy or a DV90 >15 Gy results in a beneficial long-term outcome after radioactive stenting. (J Am Coll Cardiol 2002;39:400-7) © 2002 by the American College of Cardiology

Intravascular brachytherapy has become a promising interventional approach to reduce the restenosis rate after coronary interventions. Its therapeutic effect is most probably due to the prevention of the proliferation and migration of smooth muscle cells and myofibroblasts from the media and/or the adventitia to the intima (1). The devices used so far include radioactive wire or seed sources, radioactive stents and radioactive liquid-filled balloons. However, the restenosis rates of intracoronary brachytherapy differ from study to study, depending on the source and the protocol (2). All devices (and in particular beta-particle-emitting stents) are limited by a peculiar type of restenosis at the margins of the interventional length, termed "candy-wrapper" or edge-effect (3). The clinical experience emphasizes the importance of dosimetry because underdosing will be ineffective in reducing restenosis (4) or may even stimulate cell growth (5), whereas overdosing may cause vessel damage, such as aneurysm development (6). We recently developed a computer algorithm to analyze the dose distribution in a given zone of the vessel wall by applying dose-volume histograms (DVHs) (7). Dose-volume histo-

grams, which describe the distribution of the irradiated tissue volume with respect to dose, are widely utilized for treatment planning in radiotherapy (8). Explicit values of dose-volume parameters can be extracted from the DVH data, for example, the dose delivered to at least a given percentage of the volume. In order to calculate DVHs, it is necessary to obtain information on the geometry of the vascular cross-sections. Intravascular ultrasonography (IVUS) is a well-established technique providing this information by tomographic imaging of the vessel wall. The present study was performed to test the value of IVUS-derived DVHs for determining the dose-dependency of intimal hyperplasia and vascular remodeling after implantation of radioactive P-32 stents.

METHODS

Patients. All patients were prospectively enrolled in the Vienna P-32 Dose Response study, which was designed to test the safety and efficacy of beta-particle-emitting phosphorus-32 BX stents (Isostent, Belmont, California) with an initial activity up to 888 kBq (24 μ Ci) in patients with either de novo lesions, in-stent restenoses or restenoses after balloon dilation (9). The stents were available in a length of 15 mm and a nominal diameter of 3.0 mm or 3.5 mm in the expanded mode. The study was performed in accordance with the Helsinki Declaration of 1964, as revised in 1989, and was approved by the Medical Ethics

From the *Division of Cardiology, Department of Internal Medicine II, †Department of Radiotherapy and Radiobiology and ‡Division of Biometrics, Department of Medical Computer Sciences, University of Vienna, Vienna, Austria. Supported by an educational grant from Isostent, Inc., Belmont, California, and the Hans und Blanca Moser-Stiftung, Vienna, Austria.

Manuscript received July 10, 2001; revised manuscript received October 15, 2001, accepted November 1, 2001.

Abbreviations and Acronyms

- DVH = dose-volume histogram
- DV10 = the dose of radiation delivered to at least 10% of the adventitial volume
- DV90 = the dose of radiation delivered to at least 90% of the adventitial volume
- EEL = external elastic lamina
- IIH = intrastent intimal hyperplasia
- IVUS = intravascular ultrasound
- LA = lumen area
- LDR = low-dose rate
- PA = plaque area

Committee of the University of Vienna. All patients gave written informed consent for their participation. From January to May 1999, 36 patients underwent implantation of one or two P-32 impregnated BX stents per lesion.

For this dose-response analysis we included only patients with de novo lesions without significant calcification that were treated with a single stent. In-stent restenoses (n = 6, 16.7%) or severely calcified lesions (n = 3, 8.3%) were excluded because the shielding effect from previously implanted stents or calcification cannot be exactly estimated at this time without histologic analysis. Furthermore, we excluded patients with more than one stent per lesion (n = 8, 22.2%) in order to eliminate uncertainties resulting from differences in the relative position of the stents (separate, abutting or overlapping). After the exclusion of patients for whom incomplete follow-up or IVUS documentation was available (n = 4, 11.1%), 15 patients were analyzed for this study.

Coronary intervention and IVUS imaging. Biplane coronary angiography was performed by using the Judkins technique. Before the intervention, the patients received 250 mg acetylsalicylic acid and 10,000 IU heparin intravenously. During the procedure, the activated clotting time was measured and maintained >300 s. Optimal stent

deployment was guided by IVUS (Boston Scientific Corp., Sunnyvale, California) under fluoroscopic control. Automatic pullback of the catheter was performed (0.5 mm/s), and images were recorded (s-VHS videotapes) for subsequent off-line analysis. After the intervention, the patients were treated with acetylsalicylic acid (100 mg/day, indefinitely) and ticlopidine (500 mg/day for 90 days). Coronary angiography and IVUS were performed in the same way at the six-month follow-up.

Quantitative IVUS. Data on reproducibility of our IVUS measurements have been published elsewhere (10). For geometry reconstruction, IVUS images after stent implantation and at follow-up were analyzed off-line by an experienced observer. In order to superimpose the dose-distribution grid on a longitudinal vessel geometry model, seven sections were selected by modifying a previously published method of serial IVUS analysis (11). Given the constant pull-back velocity of 0.5 mm/s, we determined the following measurement points: a cross-section 2.5 mm distal of the stent (distal peri-stent) (A), the distal stent edge (B), the first quarter (C), the center (D) and the third quarter of the stent (E), the proximal stent edge (F) and a cross-section 2.5 mm proximal of the stent (proximal peri-stent) (G) (Fig. 1). The measured frame was considered to be representative for the corresponding total section volume. The lumen area (LA) and the total vessel area were measured in end-diastolic frames by manually tracing the leading edge of the intima and the external elastic lamina (EEL), respectively. In our study, the EEL was visible and traceable in all cases. Plaque area (PA) was defined as the intima + media area and was calculated as EEL area - LA. Plaque growth was determined as the difference between PA at follow-up and postintervention (Δ PA). For the stent segments (B to F), intrastent intimal hyperplasia (IIH) was defined as stent area at follow-up - LA at follow-up. The extent of vascular remodeling was determined by Δ EEL (EEL at follow-up - EEL after stent).

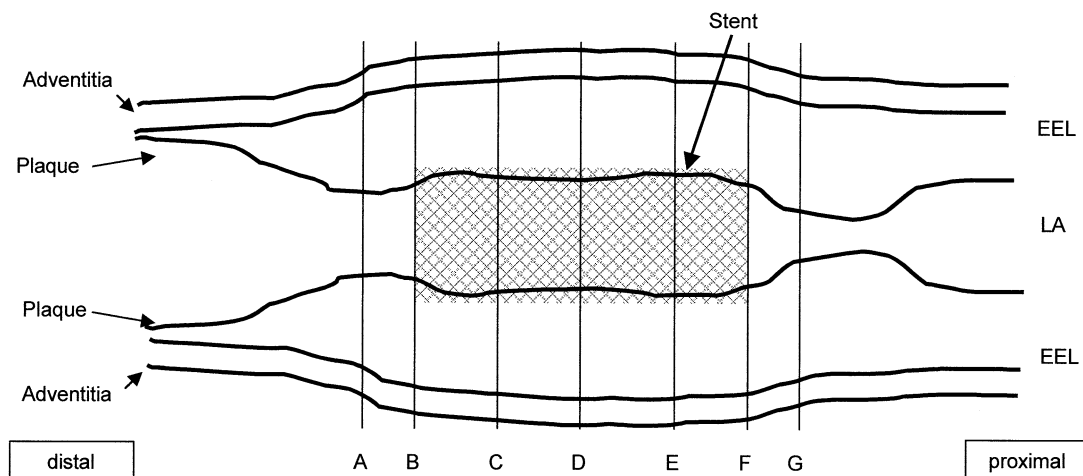


Figure 1. Schematic drawing of a stented vessel segment. For localization of the cross-sections, see the text. Atherosclerotic plaque was defined as the difference between the lumen area (LA) and the external elastic lamina (EEL) area. Intrastent intimal hyperplasia was defined as the difference between the stent area and the LA at follow-up.

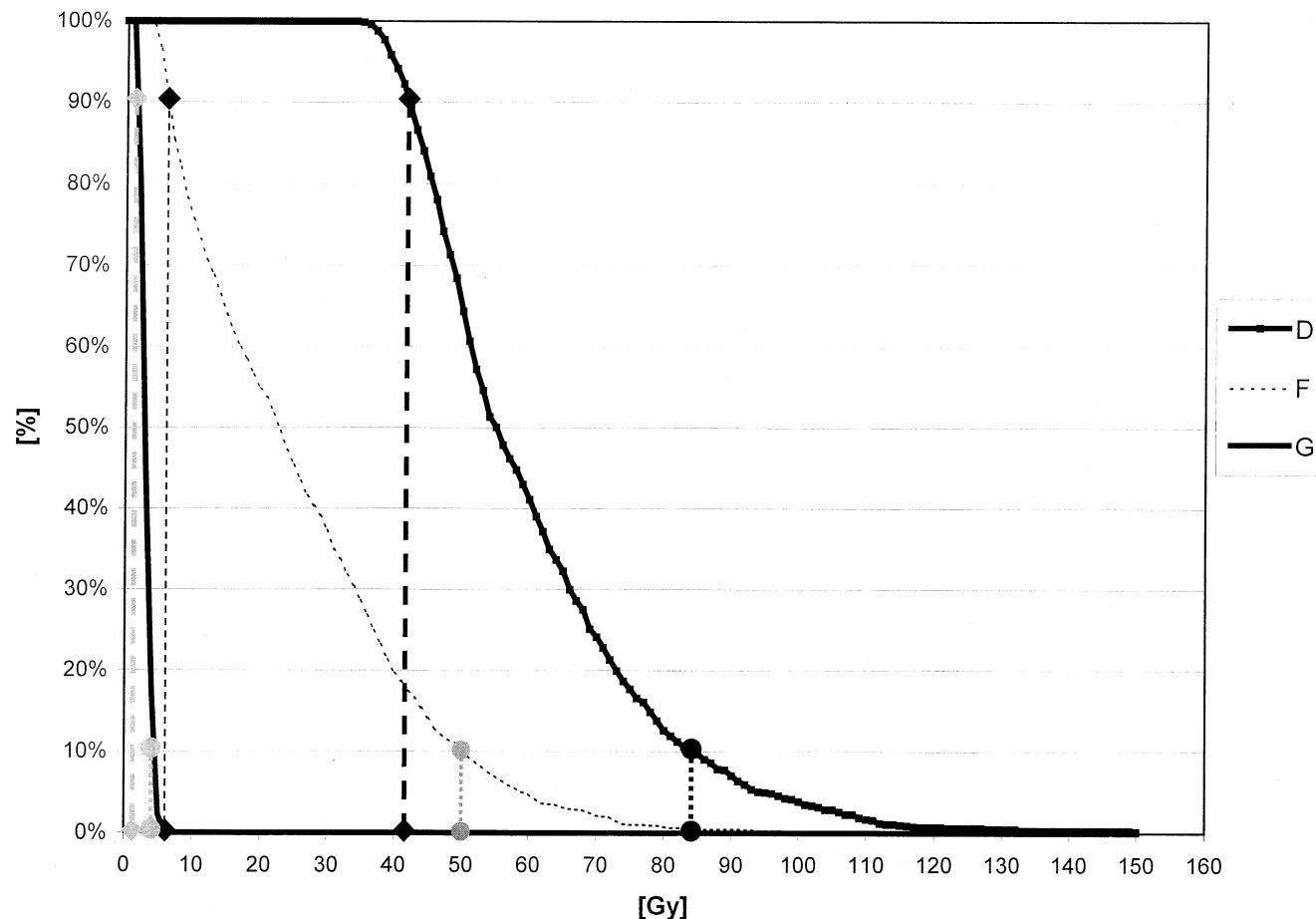


Figure 2. Cumulative dose-volume histogram of three segments from one patient receiving a radioactive stent. The ordinate represents the percentage of target volume receiving at least the respective dose shown at the abscissa. The value of DV10 is marked by a **circle** and that of DV90 by a **diamond**. Note the different decline of the curves in each segment resulting in a broad variety of delivered doses, especially of the dose of radiation delivered to at least 10% of the adventitial volume, and a high cumulative dose in the central segments.

Dosimetry. The DVH calculations used in our study are based on the dose distribution around the stent as calculated by Janicki et al. (12) for the source immersed in water as adapted to the design of the BX stent. The underlying dose map was chosen on the basis of the nominal stent diameter (3.0 mm and 3.5 mm) and the activity at the time of implantation but adapted to the real dimension of the stent once implanted as delineated by IVUS. The algorithm used in the present calculation model has been described in detail elsewhere (7). Briefly, the underlying dose map is based on the stent design and the initial activity. The algorithm used in our approach also includes the actual geometry of the stent within the vessel wall and its position related to the adventitia, the assumed target volume. The actual dose distribution within the adventitia is derived by determination of the actual distances between the stent surface and a representative amount of points within the target volume. This incorporates deviations from the nominal circular shape of the stent and vessel wall geometry. In the present work, all calculated doses are given as the cumulative dose received within 28 days after stent implantation according

to the recommendations of the American Association of Physicists in Medicine (13).

Histogram calculation. We assessed the dose distribution within the adventitia, presuming a thickness of 0.5 mm from the EEL contour (14). The digitalization of an individual IVUS section generates a two-dimensional matrix containing a polygon of the vessel lumen contour and the EEL contour with one matrix cell (voxel) representing a square of approximately $40 \times 40 \mu\text{m}$. The third dimension is obtained by including the length of the respective segment (3.0 mm or 2.5 mm) representing the Z-axis. A computer algorithm developed in our laboratory using the MATLAB 5.1 programming language (The MathWorks, Inc., Natick, Massachusetts) calculates the dose in randomly allocated voxels inside the target volume.

To calculate differential DVHs, the computer code counts the number of those voxels receiving a dose within specified equispaced dose intervals of 1 Gy. The cumulative DVH, representing the percentage of the total target volume receiving a dose greater than or equal to a given dose is derived by a summation procedure of the differential

DVHs (Fig. 2). In order to compare DVHs, the minimum doses of radiation delivered to at least 10% and 90% of the adventitial volume are presented (DV10, DV90). Whereas DV90 accounts for the therapeutic effect of radiotherapy, the higher values of DV10 determine the deleterious sequelae of irradiation. It should be noted that these values cannot be compared with the respective dose delivered by a temporary brachytherapy source because they refer to a reference volume, not only to a reference point, and because the radioactive stents have a much lower dose rate.

Statistics. Results are expressed as means ± SEM. The segmental data (LA, IHH, EEL, PA) on all patients were compared by analysis of variance. We used an unpaired *t* test in order to compare morphometric changes between high-dose (DV10 >90 Gy, DV90 >15 Gy) and low-dose (DV10 <90 Gy, DV90 <15 Gy) groups. These doses do not represent calculated threshold values but have been derived from our raw data because the morphometric changes were most evident in this range. Most protocols using intravascular catheter-based brachytherapy employ a dose of approximately 15 Gy, which, therefore, is a familiar number to most cardiologists. The threshold of DV10 has been fixed sixfold higher than that of DV90. There are, of course, differences in the biologic effect of low-dose rate (LDR) and high-dose rate irradiation with the same cumulative dose, as will be discussed later. The dose-response relationship was tested by regression analysis; the variance stabilization of the x-value was obtained by logarithmic transformation:

$$y = b^0 + b^1 \cdot \ln(x)$$

In order to avoid the bias due to serial data being obtained from the same patient, which would unwarrantedly increase the number of observations, the data on the segments displaying nonsignificant differences between the segments were averaged, and the correlation between the greatest and smallest segmental changes in intimal hyperplasia and EEL versus radiation doses (DV10 and DV90) were calculated (StatView 5.01, SAS Institute Inc, SAS Campus Drive, Cary, North Carolina). Differences were considered significant when p value was <0.05.

RESULTS

Clinical data. Fifteen patients (14 male and 1 female, mean age: 61.1 ± 2.8 years) were included in this study. Ten stents were implanted in the left anterior descending coronary artery (66.6%), one (6.6%) in the left circumflex coronary artery and four (26.7%) in the right coronary artery. Five patients (33.3%) received a 3.0-mm stent and 10 patients (77.7%) received a 3.5-mm stent (mean 3.33 ± 0.2 mm). The average stent radioactivity at the time of implantation was 426.24 ± 34.0 kBq (11.52 ± 0.9 μCi); the mean dose within 0.5 mm from the stent surface in the central plane was 107.9 ± 8.3 Gy. Four of the 15 patients (26.6%) had a significant angiographic restenosis >50% diameter stenosis at follow-up.

Table 1. Analysis of Vessel Segments

	A. Morphometric Changes Six Months After Radioactive Stent Implantation							
	A	B	C	D	E	F	G	
	Distal Persistent	Distal Stent Edge	First Stent Quarter	Stent Center	Third Stent Quarter	Proximal Stent Edge	Proximal Persistent	
ΔLA (mm ²)	-2.19 ± 0.8	-2.72 ± 0.7*	-0.81 ± 0.4	-0.49 ± 0.4	-1.22 ± 0.4	-2.98 ± 0.9*	-2.21 ± 0.7*	
ΔEEL (mm ²)	-0.12 ± 0.8†	0.46 ± 0.3†	2.47 ± 0.5	2.18 ± 0.7	1.09 ± 0.7	0.62 ± 0.9	-0.47 ± 0.6*	
ΔPA (mm ²)	1.52 ± 0.7	2.79 ± 0.6	3.28 ± 0.5	2.67 ± 0.5	2.31 ± 0.6	2.99 ± 0.9	1.74 ± 0.5	
	B. Delivered Doses							
DV10 (Gy)	6.6 ± 0.7	95.9 ± 6.5	133.2 ± 12.7‡	135.9 ± 12.6‡	110.5 ± 10.5‡	78.4 ± 5.5	6.3 ± 0.6	
DV90 (Gy)	2.4 ± 0.3	9.6 ± 0.8	47.5 ± 4.6‡	43.1 ± 4.23‡	42.9 ± 4.3‡	8.5 ± 0.7	2.3 ± 0.27	

*p < 0.05 vs. C, D, E; †p < 0.05 vs. C, D; ‡p < 0.01 vs. A, B, F, G.
DV10 = the dose of radiation delivered to at least 10% of the adventitial volume; DV90 = the dose of radiation delivered to at least 90% of the adventitial volume; Gy = Gray; EEL = external elastic lamina area; LA = lumen area; PA = plaque area.

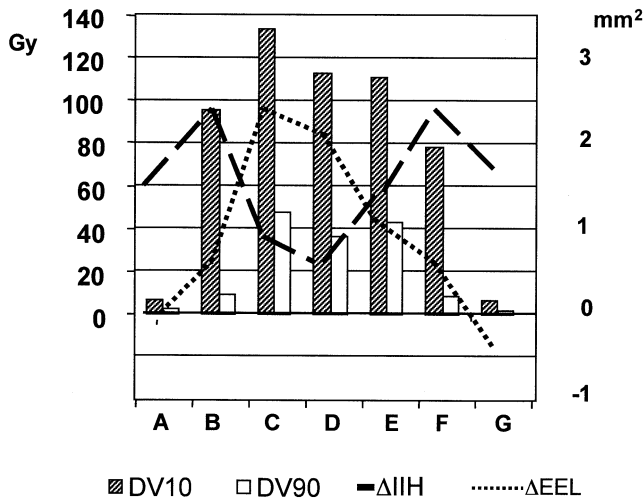


Figure 3. Comparison between the delivered dose at 10% and 90% of the adventitia (DV10, DV90), the reduction of the intimal hyperplasia and the increase in external elastic lamina (EEL) area. Note the increased intrastent intimal hyperplasia (IIH) at the stent edges. These segments absorbed lower doses than the stent body but higher doses than the peri-stent segments, which exhibit less intimal hyperplasia. Expansive remodeling occurs within the stent body but not at the edges and the peri-stent segments.

Spatial description. The morphometric changes within six months are tabulated in Table 1A. There was no significant difference between stent area after implantation and at follow-up, indicating minimal stent recoil. The DV10 and DV90 increased progressively from the stent ends to the center of the stent (Table 1B) as a consequence of the dose distribution of the BX stent. The decrease in lumen area was highest at the edges ($p = 0.029$). The analysis of the EEL showed a significant increase by up to 18% within the stent ($p = 0.016$), but no changes at the edge- and peri-stent segments. Of note, the changes in total PA did not differ between in-stent, edge and peri-stent segments; there was even a trend towards an increase in the in-stent segments. There was no correlation between any of the analyzed IVUS parameters and the initial stent activity.

Dose-dependency of IIH. Intrastent intimal hyperplasia (but not total PA) increased at the stent edges and decreased within the stent body (Fig. 3). Regression analysis between IIH and DV10 and DV90, respectively, revealed a significant logarithmic correlation (DV10: $r = 0.516$, $y = 9.90 - 1.82 \ln[x]$, $p = 0.0058$; DV90: $r = 0.617$, $y = 4.66 - 1.03 \ln[x]$, $p = 0.0005$) (Fig. 4).

Dose-dependency of vascular remodeling. The EEL was unchanged at the stent edges and increased markedly around the stent body (Fig. 3). Regression analysis demonstrated a significant logarithmic correlation between the EEL (smallest response in B and F and greatest response in segments C, D and E) and DV10 ($r = 0.476$, $y = -10.97 + 2.53 \ln[x]$, $p = 0.009$) and DV90 ($r = 0.498$, $y = -2.65 + 1.13 \ln[x]$, $p = 0.006$) (Fig. 5). The observed constriction at the peri-stent segments was not significant compared to the other segments.

Morphometric differences between high-dose and low-dose segments. Interstent intimal hyperplasia was significantly reduced in the segments that received a DV90 >15 Gy (0.8 ± 0.3 mm² vs. 2.19 ± 0.2 mm², $p < 0.001$) or a DV10 >90 Gy (1.10 ± 0.3 mm² vs. 1.93 ± 0.3 mm², $p = 0.035$). The Δ EEL was also more pronounced in segments receiving a DV90 >15 Gy (1.88 ± 0.4 mm² vs. 0.12 ± 0.4 mm², $p = 0.001$) or a DV10 >90 Gy (1.57 ± 0.3 mm² vs. 0.42 ± 0.4 mm², $p = 0.032$). However, the changes in PA did not differ between the DV90 (2.31 ± 0.4 mm² vs. 2.70 ± 0.3 mm², $p = 0.524$) and DV10 (2.35 ± 0.4 mm² vs. 2.66 ± 0.3 mm², $p = 0.436$) groups.

DISCUSSION

This study is the first to determine a dose-dependency of IIH and expansive remodeling after implantation of radioactive stents in human arteries by using IVUS-derived DVHs. Accordingly, the lumen at the stent edges is obstructed due to insufficient vessel expansion consecutive to lower doses in the presence of continuously growing neointima.

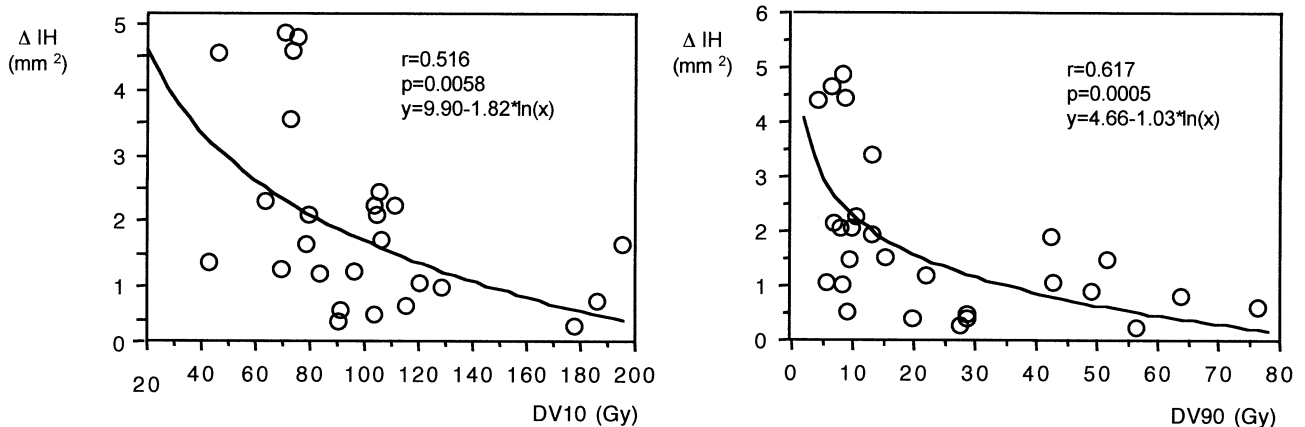


Figure 4. Logarithmic correlation between intrastent intimal hyperplasia (IIH), the dose of radiation delivered to at least 10% of the adventitial volume (DV10) and the dose of radiation delivered to at least 90% of the adventitial volume (DV90).

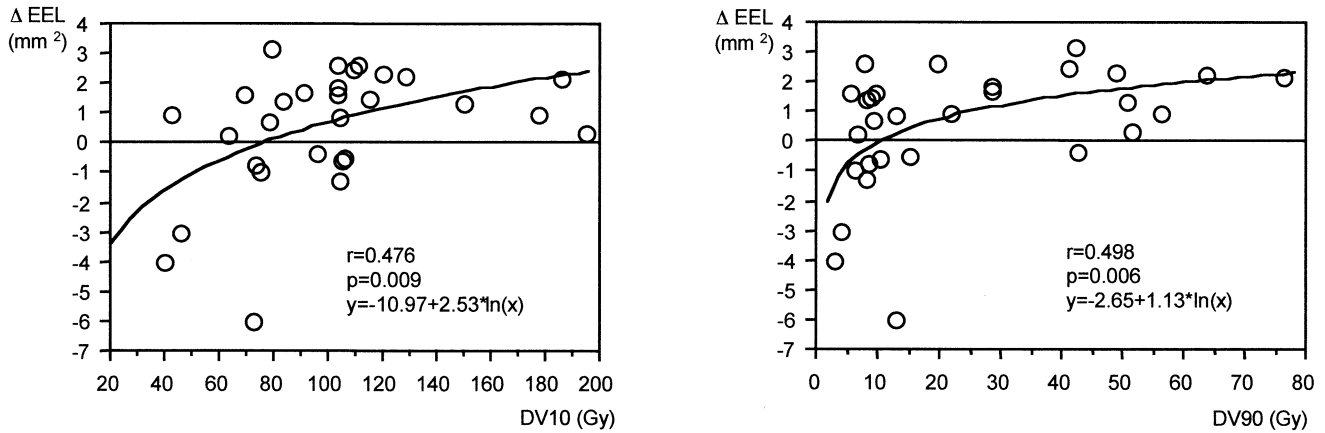


Figure 5. Logarithmic correlation between expansive remodeling (Δ external elastic lamina [EEL]), the dose of radiation delivered to at least 10% of the adventitial volume (DV10) and the dose of radiation delivered to at least 90% of the adventitial volume (DV90).

Advantage of DVHs in vascular brachytherapy. Previous investigations of radioactive stents (15,16) did not integrate the actual geometry of the treated vessel, the three-dimensional expansion of the adventitia and the apposition of the stent into their models nor did they assess the entire interventional length. Thus, it was impossible to determine a clear dose-response relation. The initial stent activity and the dose within 0.5 mm from the stent surface in the central plane alone did not correlate with morphologic changes, which creates the need for a more careful assessment of doses delivered to a defined volume. The application of DVHs, which have recently been adapted to intravascular brachytherapy (14,17,18) requires adjustment for the differences in nature between the temporary brachytherapy sources and the permanently implanted LDR sources like radioactive stents. We have recently developed an IVUS-based computer algorithm for DVHs, which accounts for the considerations mentioned in the previous text so that the dose delivered to a certain vessel layer over any given time can be calculated (7). This model allows the establishment of a radiobiologic relationship between the delivered dose and the vascular response to LDR radiation.

Morphometric changes after radioactive stenting. Our study reveals an inverse logarithmic correlation between the delivered dose and the IHH. Interestingly, we found a changing pattern of vascular remodeling along the analyzed segment over six months after the intervention; the mean increase in EEL area, which also showed a direct logarithmic correlation with the delivered dose, was about 15% within the stent, whereas it was only 6.6% at the edges and even slightly negative (-1.3%) at the peri-stent segments. The amount of intimal formation alone did not increase by >30%, even in the edge segments, which is too low to result in a significant stenosis. However, even in the stent segments without angiographic restenosis, PA increased by up to 72% due to a pronounced expansive remodeling. Thus, our study is the first to suggest a predominant role of vascular remodeling in the vascular response to radioactive stenting. Whereas vessel enlargement after temporary irra-

diation has been observed in both animals and humans (2), Kay et al. (19) did not detect an increased EEL area after radioactive stenting. This contrast may be explained by a lower activity of the stents used in their analysis (<444 kBq) because we have shown that a DV90 <15 Gy or a DV10 <90 Gy are ineffective in inducing vessel expansion. However, our data confirm the findings of Albiero et al. (20) who observed constrictive remodeling in peri-stent segments. The lack of expansive remodeling at the stent edges in the presence of constant intimal hyperplasia leads to the development of the “candy-wrapper” stenosis. Thus, the positive effect of vascular brachytherapy seems to depend on a significant increase in vessel size. The long-term outcome of radioactive stenting, therefore, is uncertain even after a satisfactory six-month result because expansive remodeling has been shown to be associated with unstable coronary syndromes (10).

Surprisingly, plaque growth was not reduced along the analyzed section. This phenomenon may be explained by the image of an “electron fence” created around the radioactive stent, which does not reduce cell proliferation but prevents cells from passing the plane of the stent struts (21). Consequently, the proliferating cells may accumulate in the abluminal vessel layers, thus increasing the vessel thickness without obstructing the lumen. Farb et al. (22) found a thickened adventitia in the presence of an increased inflammatory response and a matrix-rich intima in rabbit iliac arteries treated with radioactive stents. Furthermore, it has been shown that irradiated and, therefore, quiescent smooth muscle cells continue to synthesize elastin, which serves as a chemoattractant for monocytes (23). Another explanation may be drawn from the heterogeneity of vascular smooth muscle cells (24). It is conceivable that subpopulations with longer cell cycle times are less affected by LDR radiation from the radioactive stent due to a different radiosensitivity (25,26).

Dose-response relation of the edge effect. Our study demonstrates a logarithmic response of the vessel to the delivered doses. Considering the hypotheses described in

the previous text, neointimal hyperplasia and vascular remodeling are coupled together and, therefore, should have the same dose-dependency; if the delivered dose is insufficient to induce expansive remodeling, IHH may develop. By DVH-analysis, we estimated a DV10 above approximately 90 Gy or a DV90 above approximately 15 Gy to result in a beneficial six-month outcome of radioactive stenting. This finding is more pronounced for DV90 because it refers to a larger amount of the target volume. Due to the steep dose-decline of the beta-particle-emitting stents, the DV90 delivered to the edges is only one-fifth of that within the stent center. These values are far below the calculated threshold to induce expansion so that the continuously growing neointima can significantly obstruct the lumen. There are, of course, differences in the biologic effect of low-dose and high-dose irradiation with the same cumulative dose, as discussed previously. Therefore, the derived values may not be applicable to different treatment devices without further adaptation.

Study limitations. This analysis was retrospectively performed on a limited number of patients, which results in an only moderate correlation between the delivered dose and the vascular response. Furthermore, patients in whom the IVUS catheter could not be advanced safely were excluded. Thus, the restenosis rate in this selected group of patients (26.6%) is markedly lower than it is in the total patient cohort (42.9%) (9). However, the strict inclusion criteria of this analysis allowed the exact determination of the delivered doses without any impairment by vessel calcification, stent overlapping or side branches.

Intravascular ultrasound cannot distinguish between media and adventitia. Thus, we do not know which vessel layer was responsible for the increase in EEL observed in our study.

The determined doses are not directly measured but are derived from DVHs in an IVUS-defined target volume. The values are based on the dose distribution of P-32 with its high dose gradient, the activity at the time of the implantation and the vessel geometry as determined by IVUS. It is quite possible that the plaque composition has an impact on the dose absorption that cannot be taken into account appropriately at the moment.

The three-dimensional dose map that we used is originally based on the presumption of a circular cross-section of the stent (12). However, the cross-section of human vessels is often elliptic rather than circular. Additionally, the atherosclerotic plaque impairs the deployment of stents, so that they may not be fully expanded to their nominal diameter. Since there are only minimal differences between the calculated nominal and the actually measured stent cross-section area, it appears reasonable to use this previously reported dosimetry. The algorithm used in our approach includes the actual geometry of the stent within the vessel wall and its position related to the adventitia, the assumed target volume.

Restenosis may also occur beyond a distance of 3 mm

from the stent edge. However, the dose delivered to this zone is only minimal. Other factors might be responsible for the development of restenosis in these sections. Therefore, we excluded more remote segments from our analysis.

Hemodynamically significant restenosis is the result of extreme neointimal proliferation. The number of patients (4/15) who developed restenosis in our study was clearly too small to perform relevant statistical analysis. Therefore, we analyzed the continuous development of neointimal proliferation and remodeling instead of the end point of binary restenosis and could not determine dose differences between patients with or without restenosis.

Conclusions. The implementation of DVH reveals a dose-dependent increase of EEL area behind radioactive stents, whereas the plaque growth is not reduced but inverted into an outward direction from the stent. A calculated DV10 >90 Gy or a DV90 >15 Gy seem to have a beneficial effect on the six-month outcome of radioactive stenting. The use of isotopes with a lower dose fall-off (e.g., gamma emitters) for the development of radioactive stents could increase the DV90 in the peri-stent segments and might potentially decrease the incidence of edge-restenosis.

Reprint requests and correspondence: Dr. Paul Wexberg, Division of Cardiology, Department of Internal Medicine II, University of Vienna, Währinger Gürtel 18-20, A-1090 Vienna, Austria. E-mail: paul.wexberg@akh-wien.ac.at.

REFERENCES

1. Wilcox J, Waksman R, King S, Scott N. The role of the adventitia in the arterial response to angioplasty: the effect of intravascular radiation. *Int J Radiat Oncol Biol Phys* 1996;36:789-96.
2. Bertrand O, Lehnert S, Mongrain R, Bourassa M. Early and late effects of radiation therapy for prevention of coronary restenosis: a critical appraisal. *Heart* 1999;82:658-62.
3. Albiero R, Adamian M, Kobayashi N, et al. Short- and intermediate-term results of 32P radioactive beta-emitting stent implantation in patients with coronary artery disease: the Milan dose-response study. *Circulation* 2000;101:18-26.
4. Verin V, Urban P, Popowski Y, et al. Feasibility of intracoronary beta-irradiation to reduce restenosis after balloon angioplasty: a clinical pilot study. *Circulation* 1997;95:1138-44.
5. Joiner M, Lambin P, Malaise E, et al. Hypersensitivity to very-low single radiation doses: its relationship to the adaptive response and induced radioresistance. *Mutat Res* 1996;358:171-83.
6. Condado J, Waksman R, Gurdziel O, et al. Long-term angiographic and clinical outcome after percutaneous transluminal coronary angioplasty and intracoronary radiation therapy in humans. *Circulation* 1997;96:727-32.
7. Kirisits C, Wexberg P, Gottsauner-Wolf M, et al. Dose-volume histograms based on serial intravascular ultrasound: a calculation model for radioactive stents. *Radiother Oncol* 2001;59:329-37.
8. Drzymala R, Mohan R, Brewster L, et al. Dose-volume histograms. *Int J Radiat Oncol Biol Phys* 1991;21:71-8.
9. Wexberg P, Beran G, Sperker W, et al. Twelve month follow-up of radioactive BX stents with an initial activity of up to 24 μ Ci: the Vienna P-32 dose response study (abstr). *Am J Cardiol* 2000;86 Suppl 8A:125i.
10. Gyöngyösi M, Yang P, Hassan A, et al. Arterial remodelling of native human coronary arteries in patients with unstable angina pectoris: a prospective intravascular ultrasound study. *Heart* 1999;82:68-74.
11. Hoffmann R, Mintz GS, Popma JJ, et al. Chronic arterial responses to stent implantation: a serial intravascular ultrasound analysis of Palmaz-

- Schatz stents in native coronary arteries. *J Am Coll Cardiol* 1996;28:1134-9.
12. Janicki C, Duggan D, Coffey C, Fischell D, Fischell T. Radiation dose from a phosphorus-32 impregnated wire mesh vascular stent. *Med Phys* 1997;24:437-45.
 13. Nath R, Amols H, Coffey C, et al. Intravascular brachytherapy physics: report of the AAPM Radiation Therapy Committee Task Group No 60. *Med Phys* 1999;26:119-52.
 14. Carlier S, Marijnissen J, Coen V, et al. Guidance of intracoronary radiation therapy based on dose-volume histograms derived from quantitative intravascular ultrasound. *IEEE Trans Med Imag* 1998;17:772-8.
 15. Carter A, Jenkins S, Sweet W, et al. Dose and dose rate effects of beta-particle emitting radioactive stents in a porcine model of restenosis. *Cardiovasc Rad Med* 1999;1:327-35.
 16. Albiero R, Nishida T, Amato A, et al. Inhibition of intra-stent neointimal hyperplasia after 32P radioactive beta-particle-emitting stent implantation: IVUS and dosimetric analysis (abstr). *Circulation* 2000;102 Suppl II:II569.
 17. Carlier S, Marijnissen P, Coen V, et al. Comparison of brachytherapy strategies based on dose-volume histograms derived from quantitative intravascular ultrasound. *Cardiovasc Rad Med* 1999;1:115-24.
 18. Sabate M, Marijnissen J, Carlier S, et al. Residual plaque burden, delivered dose, and tissue composition predict 6-month outcome after balloon angioplasty and beta-radiation therapy. *Circulation* 2000;101:2472-7.
 19. Kay I, Sabate M, Costa M, et al. Positive geometric vascular remodeling is seen after catheter-based radiation followed by conventional stent implantation, but not after radioactive stent implantation. *Circulation* 2000;102:1434-9.
 20. Albiero R, Nishida T, Adamian M, et al. Edge restenosis after implantation of high activity (32)P radioactive beta-emitting stents. *Circulation* 2000;101:2454-7.
 21. Fischell T, Carter A, Laird J. The beta-particle-emitting radioisotope stent (isostent): animal studies and planned clinical trials. *Am J Cardiol* 1996;78:720-4.
 22. Farb A, Shroff S, John M, Sweet W, Virmani R. Late arterial responses (6 and 12 months) after 32P beta-emitting stent placement: sustained intimal suppression with incomplete healing. *Circulation* 2001;103:1912-9.
 23. Martin B, Ritchie A, Toselli P, Franzblau C. Elastin synthesis and accumulation in irradiated smooth muscle cell cultures. *Conn Tiss Res* 1992;28:181-9.
 24. Frid M, Aldashev A, Dempsey E, Stenmark K. Smooth muscle cells isolated from discrete compartments of the mature vascular media exhibit unique phenotypes and distinct growth capabilities. *Circ Res* 1997;81:940-52.
 25. Terasima T, Tolmach L. X-ray sensitivity and DNA synthesis in synchronous populations of HeLa cells. *Science* 1963;140:490-2.
 26. Hall E, Brenner D. The dose-rate effect revisited: radiobiological considerations of importance in radiotherapy. *Int J Radiat Oncol Biol Phys* 1991;21:1403-14.

Vascular morphometric changes after radioactivesitent implantation: a dose-response analysis

Paul Wexberg, Christian Kirisits, Mariann Gyöngyösi, Michael Gottsauner-Wolf, Meinhard Ploner, Boris Pokrajac, Richard Pötter, and Dietmar Glogar
J. Am. Coll. Cardiol. 2002;39;400-407

This information is current as of February 10, 2012

Updated Information & Services

including high-resolution figures, can be found at:
<http://content.onlinejacc.org/cgi/content/full/39/3/400>

References

This article cites 26 articles, 12 of which you can access for free at:
<http://content.onlinejacc.org/cgi/content/full/39/3/400#BIBL>

Rights & Permissions

Information about reproducing this article in parts (figures, tables) or in its entirety can be found online at:
<http://content.onlinejacc.org/misc/permissions.dtl>

Reprints

Information about ordering reprints can be found online:
<http://content.onlinejacc.org/misc/reprints.dtl>